LLNL-JRNL-2002340

Lawrence Livermore National Laboratory

Demand bidding promotes large-scale user engagement and lowers power generation cost

X Tang, M Baldea, C Petra

January 2026

Computers & Chemical Engineering

Disclaimer

This work performed under the auspices of the U.S. Department of Energy by Lawrence Livermore National Laboratory under Contract DE-AC52-07NA27344.

Demand bidding promotes large-scale user engagement and lowers power generation cost

Xin Tang[1], Cosmin G. Petra[2,*], Michael Baldea[1,3,4,**], and Ross Baldick[5]

[1]Oden Institute for Computational Engineering and Sciences, The University of Texas at Austin, Austin, TX 78712, USA
[2]Lawrence Livermore National Laboratory, Livermore, CA USA
[3]McKetta Department of Chemical Engineering, The University of Texas at Austin, Austin, TX 78712, USA
[5]Department of Electrical and Computer Engineering, The University of Texas at Austin, Austin, TX 78712, USA
[4]Lead contact
[*]Correspondence: petra1@llnl.gov
[**]Correspondence: mbaldea@che.utexas.edu

LLNL IM Release number: LLNL-JRNL-2002340

SUMMARY

We present a mechanism based on electricity demand bidding for engaging large electricity users in the operation of the power grid. We implement this concept in a grid-scale case study using a synthetic grid structure in the footprint of the grid of Texas. The results reveal that the demand bidding lowers overall power generation costs, but economic benefits decline asymptotically as the number of participants increases. Transmission line and transformer capacity constraints become the limiting factors, revealing that expanding the transmission infrastructure is key to engaging more demand-side participation. We find that demand bidding does not substantially alter the optimal operation of existing bidding entities when the number of bidders increases.

CONTEXT AND SCALE

Power grids are increasingly operating under transient conditions, largely due to the expansion of renewable energy generation. Engaging electricity users in grid operations is crucial for ensuring a balanced supply and demand at all times. Currently, user participation is mostly self-driven, with consumers scheduling electricity use based on known or predicted prices. Additionally, participation is largely voluntary, making it neither transparent nor predictable for grid operators. We introduce demand bidding as an innovative approach to enhance the predictability of large users' engagement in grid operations, while also achieving an economic equilibrium that maximizes benefits for both the grid and electricity consumers.

The simulation case is based on the Texas grid and examines, for the first time, the impact of demand bidding at the scale of an entire Independent System Operator, a scope that is far larger than any results available in the open literature. We analyze a network consisting of 534 generators, 2,000 buses, 861 transformers, and 2,345 transmission lines, solving the alternating current multi-period optimal power flow problem. The results provide unexpected insights, such as diminishing

economic benefits as user participation increases, the limiting effects of transmission infrastructure, and the relatively small impact of new users joining demand bidding programs on existing participants.

KEYWORDS

demand bidding, power grid, optimal power flow

INTRODUCTION

About one third of anthropogenic CO_2 emissions are related to electricity generation[1]. It is therefore imperative to expand the presence of renewable resources in the global power generation portfolio, and significant progress has been made in this direction. Power generation rates from wind and solar photovoltaics are highly variable across hourly, daily, and seasonal timescales. Renewable capacity expansion thus challenges the operators of the power grid, whose chief mission is to ensure that electricity supply meets electricity demand (itself highly variable) at all times.

Recognizing that renewable resources are only down-dispatchable, with energy availability generally less than nameplate capacity, the aforementioned challenges can be addressed by shifting power availability using energy storage and/or by shifting demand. The installation and operation costs of energy storage systems that have sufficient capacity to meaningfully impact the operation of the grid remain high[2] in spite of recent technology advances[3,4]. Shifting demand and demand-side management strategies consist of incentivizing users to adjust their electricity consumption patterns over time. This can be done via, *e.g.*, time of use electricity pricing, or by providing payments in return for reducing demand when requested by the grid operator[5,6]. Industrial electricity users are particularly favored for engagement in such programs, given that they present large, localized electrical loads that are largely independent of daily and seasonal changes in human preferences and schedules (unlike, *e.g.*, residential homes and commercial buildings).

Industrial demand response initiatives can in principle improve grid reliability and resource efficiency in energy production[7,8]. Participation in these programs is, however, voluntary. While users are economically *incentivized* to reduce their electricity demand at times when generation capacity is limited (or when overall demand is at a peak), they are not *obligated* to do so. It is thus reasonable to consider that these loads remain largely undispatchable and unpredictable, given that their main purpose is to make their own product(s) and meet their own market demand. Additionally, if many users simultaneously act on the same electricity price information, they are likely to both simultaneously decrease their electricity demand (to unnecessarily low levels), followed by simultaneously increasing their demand at a later time to make up for lost production. This can in turn give rise to a new peak in electricity demand (termed rebound peak), with detrimental consequences on balancing electricity consumption and generation in the grid.

Demand bidding is an emerging paradigm for demand side management, whereby large electricity users are treated akin to (the demand-side version of) generators[9]. Generators operate in an electricity market, where they have the opportunity

to offer (bid) generation capacity and specify the corresponding unit price (dollars/MWh), typically at hourly intervals over the course of a time horizon (usually 24 hours) in the future. The market is cleared (*i.g.*, prices are settled and production is allocated to each generator) at a pre-set time each day.

In demand bidding, rather than rely on (the forecasts of) electricity prices to make decisions regarding production, users submit time-dependent requests (bids) for electricity consumption (specifying required power level and price they are willing to pay). This approach enables users to directly participate in the electricity market and potentially set the market price. From a grid perspective, demand bidding provides a mechanism for managing demand more reliably and allows for increased transparency and predictability in the behavior of large users. In turn, this can increase the capacity of the grid to absorb and utilize electricity generated by renewable sources.

Existing work on demand bidding (*e.g.*, Li et al.[9], Ruan et al.[10], and Mohsenian-Rad[11]), whether focusing on the day-ahead or real-time market, assumes that the loads are market participants that (i) are too small to affect prices (*i.e.*, price takers in the sense of economics), and (ii) have a forecast of future prices. This allows a load to schedule its operation over a certain time horizon to maximize an economic criterion based on the price forecast. Kohansal et al.[12] proposed a general scenario-based stochastic optimization framework for price-maker economic bidding. In our recent work[13], we posited that demand bidding should be used to maximize a welfare function (*i.e.*, benefit all participants in the electricity market) defined by the difference between revenue obtained from selling bidding entity products and the total cost of generating power over the time horizon considered. Under this paradigm, large users contribute to price formation and are rewarded through lower energy costs accordingly for their efforts in supporting grid operations. Currently, U.S. Independent System Operators (ISOs) provide certain mechanisms for demand bidding market participation, such as the market formulation by the Midcontinent ISO (MISO)[14]. However, these mechanisms lack harmonization across ISOs, often involve complex administrative and metrology requirements, and may not incorporate essential design features for scheduling electricity consumption in industrial processes. For example, they might not include constraints to ensure adequate electricity delivery to plants over a day or support long-term scheduling for multi-day operations or labor planning, which could hinder participant engagement.

To the best of our knowledge, demand bidding concepts have been tested with relatively small systems (*e.g.*, 200-2000 variables in[12]), that are conceptually representative of but not practically relevant for existing power grids. Nevertheless, these studies (*e.g.*, Tang et al.[13]) have revealed that demand bidding by a single entity can have grid-wide effects, altering the optimal operation of generators and batteries that are not necessarily proximate to the load.

Motivated by the above, in this work we report on the results of a grid-scale case study aimed at probing the impact of demand bidding. We present a mechanism for demand bidding based on a novel multi-period (MP) alternating current (AC) optimal power flow (OPF) problem formulation. We use a synthetic grid structure in the footprint of the system operated by the Electricity Reliability Council of Texas (ERCOT) to explore grid-wide effects associated with increasing the presence of bidding loads (as a proportion of the total system load). Our results reveal that the economic benefits of demand bidding decline asymptotically as the proportion of qualified entities that engage in such programs increases. Transmission line

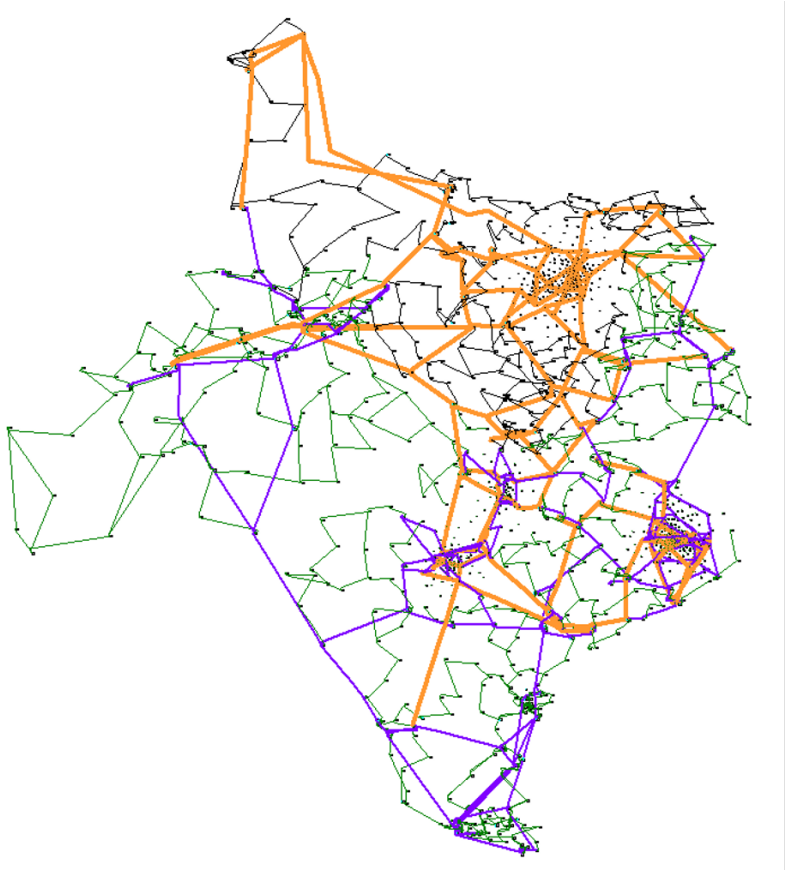

Figure 1: A 2000-bus synthetic grid on the footprint of Texas[15–18]. The orange thickened lines, purple lines, black lines, and green lines represent 500, 230, 161 and 115 kV transmission lines respectively. The black squares indicate buses.

and transformer capacity constraints become the limiting factors, revealing that expanding the transmission infrastructure is key to engaging more demand-side participation. At the same time, we find that demand bidding does not substantially alter the optimal operation of other existing bidding entities when the number of bidders increases (along with the corresponding load).

RESULTS

A mechanism for users to submit electricity demand bids

The power grid is a network of power generators, transformers, transmission lines, and buses where users with different and time-varying power demands are connected (Figure 1). The operational goal is to ensure that power supply equals power demand at any time instant, and that this goal is met at a minimum cost (typically computed over a finite time horizon $\mathcal{H}$). The degrees of freedom typically available to meet the operational goal are the power generation levels of each of the connected generators. The cost comprises variable costs related to power generation, operating personnel, etc.

Grid operators address this task by formulating and solving an optimization problem referred to as the Optimal Power Flow (OPF) problem (Equation 1).

$$\min_{P_g} \quad \text{total generation cost} \tag{1a}$$

$$\begin{aligned}
\text{subject to} \quad & \text{power supply = power demand} && \text{at each bus} \quad : \lambda && \text{(1b)} \\
& P_g{}^{min} \leq P_g \leq P_g{}^{max} && \text{for all generators} && \text{(1c)} \\
& \text{power transmitted} \leq \text{maximum capacity} && \text{for all lines} && \text{(1d)} \\
& \text{total generation cost} = && && \\
& \qquad \text{integral of} (P_g \cdot \text{generation cost}) && \text{for } \mathcal{H} && \text{(1e)}
\end{aligned}$$

In addition to the constraint on meeting power demand at all buses (Equation 1b), the OPF includes upper and lower limits on generation rates by each generator (Equation 1c), as well as capacity limits on transmission lines (Equation 1d). Additional constraints on the speed of change of generation rates in time (ramp rates), thermal limits on equipment such as transformers, etc. can be included. We adopt a multi-period (MP) alternating current (AC) OPF problem formulation, based on the single-period security-constrained AC OPF setup introduced by ARPA-E[19]. The structure of the OPF problem is illustrated in the EXPERIMENTAL PROCEDURES Section. A full model description is available in references[19,20].

The solution $P_g{}^*$ provides the generation rate for each generator at each time point in the time horizon $\mathcal{H}$. The Lagrange multiplier λ of the power balance constraint at each bus (Equation 1b) represents the locational marginal price (LMP). The LMP reflects the cost of delivering one unit of electrical energy at the corresponding bus, and is assumed to be the price to be paid by a user connected to that bus. This price is utilized by each participant to determine their production schedules by solving an optimization problem of the type:

$$\min_{\mathcal{P}} \quad \text{total electricity cost} \tag{2a}$$

$$\begin{aligned}
\text{subject to} \quad & \text{total production} \geq \text{product demand} && \text{for } \mathcal{H} && \text{(2b)} \\
& \text{production rate} = \mathcal{P} \cdot \text{production system efficiency} && && \text{(2c)} \\
& \text{total production} = \text{integral of production rate} && \text{for } \mathcal{H} && \text{(2d)} \\
& \text{total electricity cost} = \text{integral of } (\mathcal{P} \cdot \lambda) && \text{for } \mathcal{H} && \text{(2e)}
\end{aligned}$$

The LMP is reflected in the total electricity cost (Equation 2e), which is also assumed to reflect the total production cost in this case. The solution $\mathcal{P}^*$ then represents the power demand schedule of the user over the time horizon $\mathcal{H}$, which in turn dictates the production schedule. These participants therefore self-schedule their production, and are key to what is referred to as "demand response (DR)," a demand-side participation mechanism comprising short-term change in operational patterns or schedules of electricity users (the demand) in response to electricity prices.

The OPF (Equation 1) and DR (Equation 2) problems can be viewed as a leader-follower (Stackelberg) game. This game admits an equilibrium, i.e., a pair of solutions $(P_g{}^*, \mathcal{P}^*)$ where both the leader (the grid) and the followers (the electricity users) maximize their benefit. Under certain assumptions (notably, the convexity of the OPF (Equation 1) and DR (Equation 2) problems), this equilibrium is unique[21,22]. However, when a non-convex AC OPF (Equation 1) is considered,

the Stackelberg equilibrium must be determined computationally using an iterative procedure (alternating between solving the OPF for the leader and the DR problem for the followers) and its uniqueness cannot be proved analytically[23].

In contrast to the *sequential* nature of this Stackelberg game, demand bidding (DB) aims to *simultaneously* maximize benefits for both the grid and the users. This is achieved by solving an optimization problem of the form:

$$
\begin{aligned}
\min_{P_g, \mathcal{P}} \quad & \text{total generation cost} - \text{production revenue} && && \text{(3a)}\\
\text{subject to} \quad & \text{power supply = power demand} && \text{at all buses} && \text{(3b)}\\
& P_g{}^{min} \leq P_g \leq P_g{}^{max} \qquad \text{for all generators} && && \text{(3c)}\\
& \text{power transmitted} \leq \text{maximum capacity} && \text{for all lines} && \text{(3d)}\\
& \text{total generation cost} = && && \\
& \qquad \text{integral of} (P_g \cdot \text{generation cost}) && \text{for } \mathcal{H} && \text{(3e)}\\
& \text{total production} \geq \text{product demand} && \text{for } \mathcal{H} && \text{(3f)}\\
& \text{production rate} = \mathcal{P} \cdot \text{production system efficiency} && && \text{(3g)}\\
& \text{total production} = \text{integral of production rate} && \text{for } \mathcal{H} && \text{(3h)}\\
& \text{production revenue} = && && \\
& \qquad \text{total production} \cdot \text{product price} && && \text{(3i)}
\end{aligned}
$$

The objective (Equation 3a) captures the welfare of the overall system, subject to the combined constraints of the OPF and DR problems. The bidding aspect consists of treating generators and users/loads in a uniform manner. In DB, both types of entities achieve the optimal tradeoff between power (via the generation rates P_g, and consumption rates $\mathcal{P}$, respectively) and cost (represented by the two elements of the objective function), while satisfying demand constraints for power (Equations 3b) and manufactured product (Equation 3h). Operational constraints specific to each system are accounted for. The solution $[P_g\ \mathcal{P}]^*$ of (Equation 3) thus naturally represents an equilibrium where the benefits of the grid (lowest generation cost) and users (lowest production cost) are maximized.

A case study in the footprint of the Texas grid

A synthetic grid that follows the footprint of the U.S. State of Texas and approximately mimics its transmission system (with 500, 230, 161, and 115 kV transmission lines) is used[15–18]. The network consists of 2000 buses, 1350 loads, 2345 lines, 861 transformers, and 544 generators (432 of which are active during the time horizon considered), as shown in Figure 1. We consider a time horizon $\mathcal{H}$ of 24 hours with hourly time intervals t. Unit commitment decisions are not included (meaning that generators are not turned on or off, but rather their generation rates can vary between a minimum and a maximum level). The cost of generating electricity for each generator varies as a function of the generation rate, as described in the EXPERIMENTAL PROCEDURES section.

Several generation cost scenarios are considered (ranging from “cheap” to “expensive”, with the former reflecting a high presence of renewables and the latter being representative of a predominantly fossil fuel-based generation portfolio). An

AC representation is used, including thermal limits and power flow constraints for transmission lines and transformers. The formulation details are included in the EXPERIMENTAL PROCEDURES Section.

The load (electricity demand) is modeled after data gathered from the Texas grid operator, ERCOT[17,18]. The synthetic grid is divided into eight zones that reflect the geographical distribution of the ERCOT grid. A year-long total demand signal with hourly time intervals is defined for each zone based on the corresponding ERCOT demand data. The hourly load at each bus is computed by using a load distribution ratio based on a snapshot of bus load distribution taken at a reference time. The total load of the system ranges between 25,379 MW and 72,903 MW. The model is agnostic to the type of load (residential, commercial or industrial).

We model industrial entities that engage in demand bidding in a similar fashion as Tang et al.[13], who considered a chlor-alkali plant with a nominal load of 50 MW as a prototypical large electric load. Bidding load information includes maximum and minimum power demand values (35 MW and 70 MW, respectively), process efficiency, unit revenue and production ramping limits as described in Equation 3 and in the EXPERIMENTAL PROCEDURES section.

The buses with the largest minimum hourly load (throughout the year) are selected as candidates for locating bidding entities. A bidding entity is assumed to *replace* (a portion of) the existing load, up to the maximum power demand of 70 MW. We also assume that there is at most one bidding entity per bus.

In our numerical experiments, the number of bidding entities is increased gradually, starting from the highest load bus and continuing to the next highest, etc. For the purpose of quantifying the evolution of this process, we introduce the bidding ratio R_b as the ratio of the total nominal load of the bidding entities and the minimum yearly grid load. Specifically:

$$R_b = \frac{\text{Number of bidding entities} \cdot \text{Nominal load}}{\text{25,379 MW}} \tag{4}$$

The increase of R_b is studied in two circumstances: with and without transmission line and transformer constraints. The intent in the latter case is to discern the impact of the grid structure on demand bidding. Eliminating transmission line and transformer constraints amounts to approximating the entire grid as being connected to a single bus with infinite transmission capacity.

The synthetic grid model[17,18] originally includes 118 generators with zero generation cost (out of 544 generators). Specifically, the generation cost is zero regardless of the power generation levels. In our study, we consider these 118 generators under two economic circumstances: the original, zero-cost case, and a case where the generation cost is non-zero, *i.e.*, linearly increasing costs from 0 $/MWh to 1000 $/MWh over the nameplate capacity of the generators, which allows us to probe the impact of demand bidding on the operation patterns of generation resources as a function of cost.

For the purpose of this study, a subset of 15 days was selected from the year-long data set. One day was selected randomly from each calendar month. Two days corresponding to the overall minimum and maximum daily *energy* demand (days 87 and 224, respectively), and one day (day 95) corresponding to the overall minimum power demand, were included in the set to capture extreme conditions (Note that day 224 was also the day of maximum overall power demand).

Demand bidding lowers overall generation cost

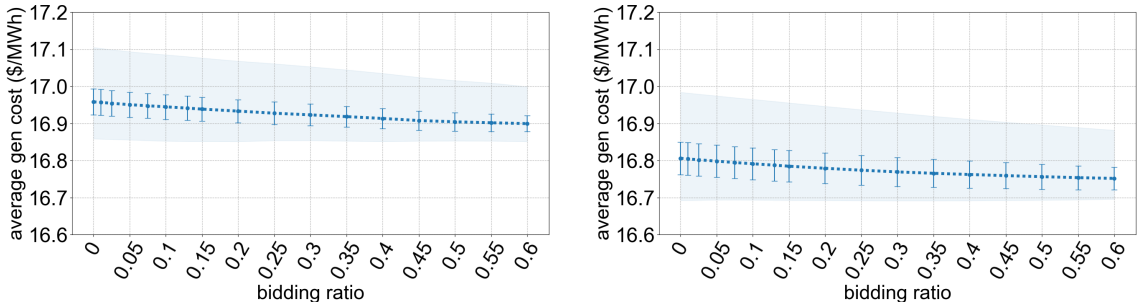

(a) (b)

Figure 2: Generation cost for the maximum energy demand day (day 224) in the transmission-constrained case (a) and unconstrained case (b). The shaded area represents the range of generation costs for all generators, while the mean is represented by the dashed line. The whiskers capture the standard deviation.

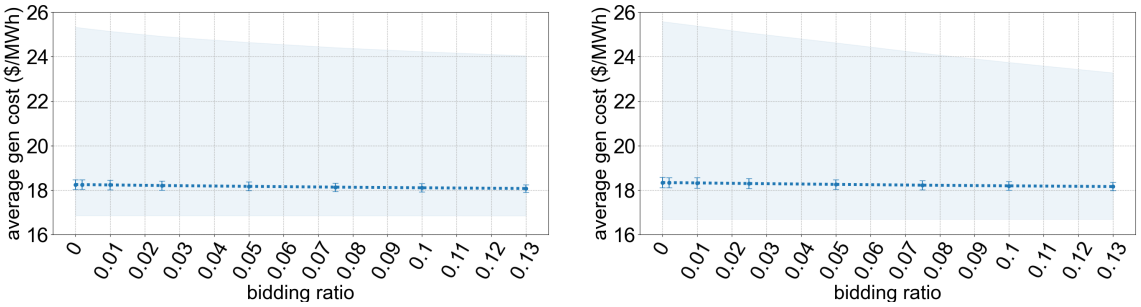

Figure 3: Average generation costs in the transmission-constrained case (a) and unconstrained case (b). The shaded area represents the range of generation costs for all generators, while the mean is represented by the dashed line. The whiskers capture the standard deviation.

We observe that increasing the bidding ratio R_b results in decreasing the overall generation cost (Figure 2). This effect is more pronounced when there are no transmission constraints (Figure 2b), an intuitive result given that in this case power can be delivered as needed, from any generator to any load. The generation cost benefits of increasing the bidding ratio R_b appear to plateau once $R_b > 0.4$ in both cases, since system flexibility is limited by generator capacity and transmission constraints.

The observations above pertain to the highest-load day (Figure 2), but are valid for all the days in our study, as shown in Figure 3 (where the generation cost of the zero-cost generators was set to zero). We point out that on some days the number of buses with loads large enough to be replaced by the bidding entity we described above was quite low, which limited the value to which R_b could be increased. For day 87 (lowest overall energy demand), the maximum achievable bidding ratio was $R_b = 0.13$, and the data for all days are plotted up to this value only.

Demand bidding provides load shifting without rebound peaks

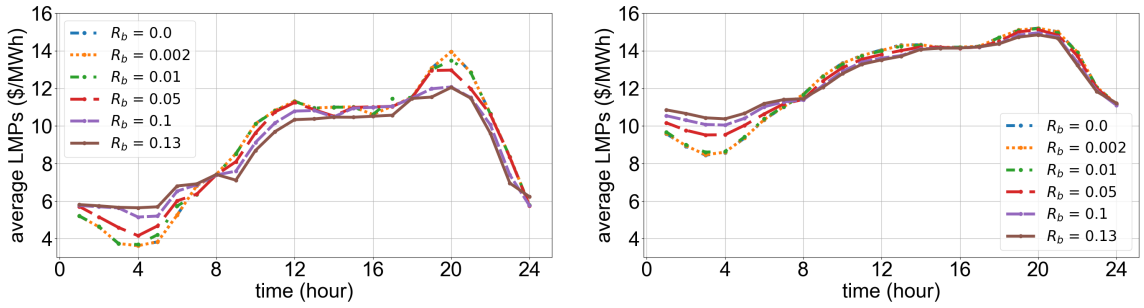

(a) (b)

Figure 4: Hourly average (over all buses and all days) locational marginal price (LMP) profiles as a function of the bidding ratio R_b for the case of zero (a) and non-zero (b) unit generation cost for the 118 originally zero-cost generators. Transmission-constrained scenario.

The observations above confirm that demand bidding reduces overall generation cost. Here, we zoom in on its daily impact. As seen in Figure 4, increasing the bidding ratio has a "peak-shaving" and "valley-filling" effect. That is, locational marginal prices during peak hours are reduced, while prices during off-peak hours increase. This effect is less pronounced when the cost of power generation increases (Figure 4), which can be explained by the fact that the impact of generation rates on cost is lower and there are thus fewer degrees of freedom available to lower overall cost.

We also note that there are no apparent rebound peaks in the cost profiles, which attests to the fact that an equilibrium is reached between the leader and follower entities as described above.

Increased demand bidding does not substantially alter the behavior of participating entities

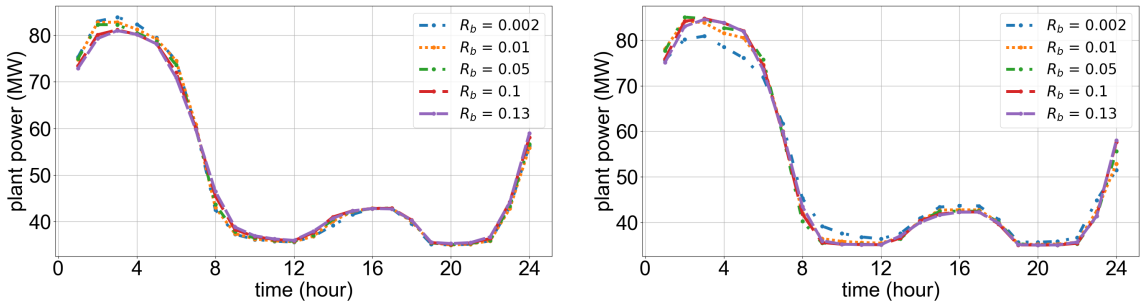

(a) With transmission constraints (b) Without transmission constraints

Figure 5: Average power demand profiles for the bidding loads as a function of R_b assuming zero-cost generators are present, with and without transmission constraints.

Figure 5 shows the average power demand profiles of the demand bidding entities for each of the 15 days considered in the study. We note that these profiles do

not change substantially as the bidding ratio increases, suggesting that the operation (*i.e.*, production schedules) of the entities that *already* use demand bidding are not impacted much by *other additional entities* engaging in demand bidding. The changes in demand profile are more pronounced during the early hours of the day, and more evident for the transmission constrained case. This can be explained by the fact that (other) grid demand is at its lowest during this time interval, and as a consequence there is more flexibility for large industrial loads to operate. The patterns revealed in this figure are consistent with the discussion provided for Figure 4, in that they show that the bidding ratio has a peak shaving effect on the bidding entities themselves.

Transmission capacity limits the benefits of demand-side participation

Figures 6, 7, 8, and 9 help visualize the constraints related to transmission lines and transformers. As the bidding ratio increases (in the interest of clarity, we only show the cases of $R_b = 0$ and $R_b = 0.13$ for Day 1, cases of $R_b = 0.4$ and $R_b = 0.45$ are added for Day 224 to show the plateau), the set of active constraints changes as well. The data indicate that the number of active constraints changes substantially up to a certain point ($R_b > 0.4$ in this case study), demonstrating that transmission and transformer capacity constraints are key limitations in expanding the benefits of demand bidding. The results shown in the figure only reflect one day of operation (Day 1 or Day 224) but similar effects were observed for all the other days.

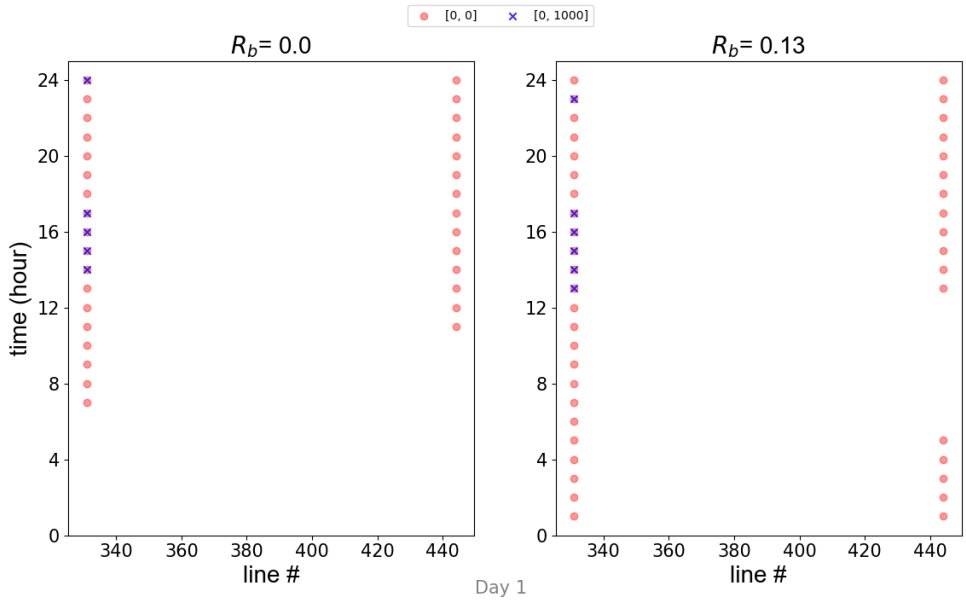

Figure 6: Evolution of active transmission line constraints as a function of bidding ratio R_b for Day 1. The case of zero-cost generators is shown in red circles, whereas the case of non-zero cost generators is shown in blue crosses. For a given transmission line (abscissa), the presence of a circle or a cross means that the line power transmission capacity constraint is active at a given time interval (shown on the ordinate).

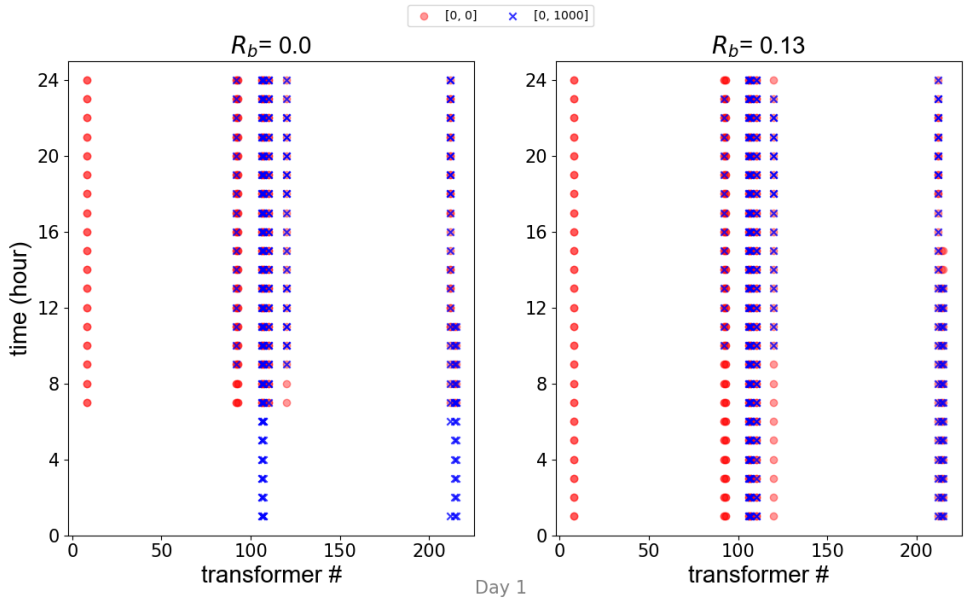

Figure 7: Evolution of active transformer capacity constraints as a function of bidding ratio R_b for Day 1. The case of zero-cost generators is shown in red circles, whereas the case of non-zero cost generators is shown in blue crosses. For a given transformer line (abscissa), the presence of a circle or a cross means that the transformer maximum power constraint is active at a given time interval (shown on the ordinate).

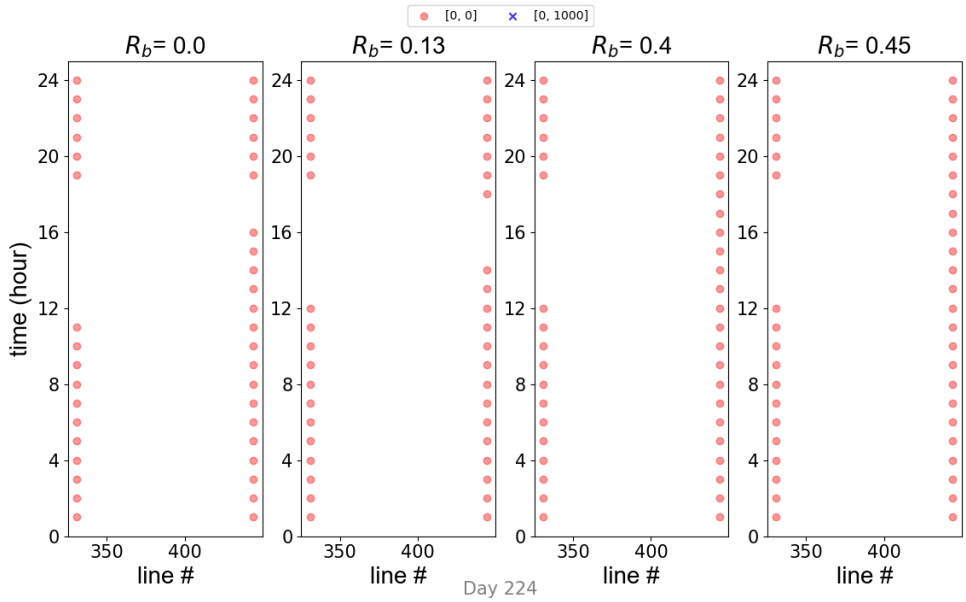

Figure 8: Evolution of active transmission constraints as a function of bidding ratio R_b for Day 224. The case of zero-cost generators is shown in red circles, whereas the case of non-zero cost generators is shown in blue crosses. For a given transmission line (abscissa), the presence of a circle or a cross means that the line power transmission capacity constraint is active at a given time interval (shown on the ordinate).

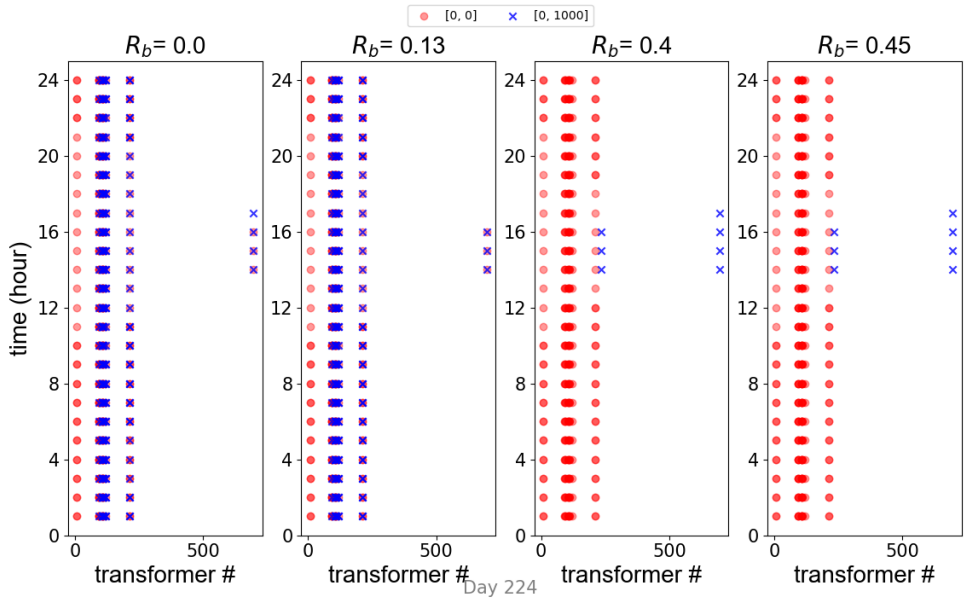

Figure 9: Evolution of active transformer capacity constraints as a function of bidding ratio R_b for Day 224. The case of zero-cost generators is shown in red circles, whereas the case of non-zero cost generators is shown in blue crosses. For a given transformer line (abscissa), the presence of a circle or a cross means that the transformer maximum power constraint is active at a given time interval (shown on the ordinate).

DISCUSSION

This is the first (to our knowledge) study to explore the impact of demand bidding on the operation of the power grid at a practically relevant scale. As a mechanism for demand-side participation, demand bidding is a natural way to reach an equilibrium between two entities - the grid (as the leader) and the electricity users (the followers). The demand bidding mechanism proposed here is based on a modified formulation of the optimal power flow problem, and aims to maximize an overall welfare function. It has the benefit of converging to an equilibrium, assuming that the problem is feasible, without requiring an iterative procedure as has been discussed in the literature.

The numerical study performed here reveals several benefits of demand bidding. First, it reduces the overall power generation cost by about 1% (whether transmission constraints are present or not). Second, it avoids the recognized disadvantages of other demand-side participation approaches, such as the appearance of rebound peaks in demand. These results are not unexpected. However, our study provides several unique and remarkable insights. First, the benefits of demand bidding tend to wane as the proportion of eligible users that choose to participate (*i.e.*, the bidding ratio R_b increases. The implication of this finding is that there is no incentive for (or no need to) expand such demand-side participation beyond a certain number of users, or to seek the engagement of all eligible users. Second, engagement on the side of the users themselves is likely to be uneventful relative to e.g., demand response, in the sense that the operating patterns will likely not be significantly different. More importantly, the operating patterns of

bidding entities are unlikely to be significantly affected by the participation of *other* entities in demand bidding. In other words, a user can remain confident that their own operations will not be significantly affected by *future* adopters joining the demand bidding program. Last but not least, the computational results provide a path for planning grid capacity expansion, particularly in terms of fortifying transmission lines and transformers. Studies that simultaneously dispatch generation capacity and demand flexibility, like this one, can reveal the lines and transformers that are expected to represent bottlenecks in the expansion of demand-side participation programs, and that should be prioritized for upgrade and/or replacement by grid operators and utilities.

Limitations of the study

The present study does not consider unit commitment decisions, which are an important part of grid operations. Specifically, unit commitment decisions pertain to timing the shut-down and start-up cycles of generators, and include considerations related to start-up timing from a "cold" or "warm" condition, minimum downtime between shut-down and start-up, etc. These considerations involve binary decisions, which complicate the problem in Equation 1. Nevertheless, we believe that our findings are broadly valid and would remain true if unit commitment were to be taken into account.

We assume that the bidding entity generates a single saleable product (in this case, chlorine). Nevertheless, there are practical cases where this entity may generate multiple products (each with its own price and energy consumption characteristics) subject to some overall energy and material balance constraints. Accounting for these features would complicate the optimization problem in Equation 3, but we believe that the findings of our study would not be fundamentally different.

Our models of the bidding entity do not explicitly account for any equipment constraints (although a ramp rate constraint is imposed to limit the speed at which process parameters can change). In practice, it is likely that more elaborate/detailed constraints should be included to reflect specific concerns regarding the impact of highly variable operation on equipment wear and tear or service life.

We also recognize that the demand bidding problem (Equation 3) does involve a level of information exchange between the leader and follower entities (including information regarding product demand, product price and process efficiency) that is currently not the norm in industry. However, we believe that this exchange can occur with the appropriate protections in place, that obfuscate this information from the public and exempt it from disclosure.

EXPERIMENTAL PROCEDURES

Demand bidding AC OPF formulation

The basis for formulating the demand bidding problem (Equation (3)) is a multi-period AC OPF. In turn, this problem is constructed by extending the single-period security-constrained AC OPF formulation described in detail in[19]. The model is described conceptually below.

In this model, the objective function to be minimized is a summation of generation GC and penalty costs PC (5b). This setup allows for real and reactive power nodal violations, as well as branch (transmission line and transformer) overloading, which are penalized at costs that are much higher than operating costs. The penalties (σ) are summed (according to (5i) with coefficients calculated from input data). The operating cost is the sum of the generation cost of all generators ((5h), where GC_g is calculated using (7)) as described later. Decision variables including active and reactive generation rates (P_g, Q_g) for all generators ($\mathcal{G}$), as well as active and reactive branch power flows at origin (P_{e_1}, Q_{e_1}) and destination (P_{e_2}, Q_{e_2}) bus e, for all e in the set $\mathcal{B}$ of lines and transformers. Voltage magnitude v_n and angle θ_n at each bus n in the set $\mathcal{N}$ are also decision variables. All the variables are bounded by minimum and maximum capacities as shown in Equations (5j) to (5o). Finally, our AC OPF formulation includes soft constraint violation: $\sigma_{a,n}, \sigma_{r,n}$ for active and reactive power balances at each $n \in \mathcal{N}$, and $\sigma_{e_1}, \sigma_{e_2}$ for line/transformer thermal limit constraints for each $e \in \mathcal{B}$. We denote the vector of all these decision variables generically by x.

$$
\begin{aligned}
\min_{x=\{P_g,Q_g,v_n,\theta_e,\sigma\}} \quad & f(x) && \text{(5a)}\\
s.t. \quad & f(x) = GC(x) + PC(x) && \text{(5b)}\\
& P_{a,n}(x) = \sum_{g\in\mathcal{G}(n)} P_g - P_{D,n} - G_n^S v_n^2 - \sum_{e\in\mathcal{B}(n)} P_e = \sigma_{a,n} \quad \forall\, n \in \mathcal{N} && \text{(5c)}\\
& Q_{r,n}(x) = \sum_{g\in\mathcal{G}(n)} Q_g - Q_{D,n} - B_n^S v_n^2 - \sum_{e\in\mathcal{B}(n)} Q_e = \sigma_{r,n} \quad \forall\, n \in \mathcal{N} && \text{(5d)}\\
& P_{e_i} = P_{a,e}(x) = P^A v_{e_i}^2 + P^B v_{e_i} v_{e_{3-i}} \cos(\theta_e) + P^C v_{e_i} v_{e_{3-i}} \sin(\theta_e) \\
& \qquad \forall\, e \in \mathcal{B}, i \in \{1,2\} && \text{(5e)}\\
& Q_{e_i} = Q_{r,e}(x) = Q^A v_{e_i}^2 + Q^B v_{e_i} v_{e_{3-i}} \cos(\theta_e) + Q^C v_{e_i} v_{e_{3-i}} \sin(\theta_e) \\
& \qquad \forall\, e \in \mathcal{B}, i \in \{1,2\} && \text{(5f)}\\
& P_{e_i}^2 + Q_{e_i}^2 \le (R v_{e_i} + \sigma_{e_i})^2 \quad \forall\, e \in \mathcal{B}, i \in \{1,2\} && \text{(5g)}\\
& GC(x) = \sum_{g\in\mathcal{G}} GC_g && \text{(5h)}\\
& PC(x) = C(\sigma) = \sum_{n\in\mathcal{N}} \left(PC^A \sigma_{a,n}^2 + PC^B \sigma_{a,n} + PC^A \sigma_{r,n}^2 + PC^B \sigma_{r,n} \right) \\
& \qquad + \sum_{\substack{e\in\mathcal{B}\\ i\in\{1,2\}}} \left(PC^A \sigma_{e_i}^2 + PC^B \sigma_{e_i} \right) && \text{(5i)}\\
& P_g^{min} \le P_g \le P_g^{max} \quad \forall\, g \in \mathcal{G} && \text{(5j)}\\
& Q_g^{min} \le Q_g \le Q_g^{max} \quad \forall\, g \in \mathcal{G} && \text{(5k)}\\
& P_{e_i}^{min} \le P_{e_i} \le P_{e_i}^{max} \quad \forall\, e \in \mathcal{B}, i \in \{1,2\} && \text{(5l)}\\
& Q_{e_i}^{min} \le Q_{e_i} \le Q_{e_i}^{max} \quad \forall\, e \in \mathcal{B}, i \in \{1,2\} && \text{(5m)}\\
& v_n^{min} \le v_n \le v_n^{max} \quad \forall\, n \in \mathcal{N} && \text{(5n)}\\
& \theta_n^{min} \le \theta_n \le \theta_n^{max} \quad \forall\, N \in \mathcal{N} && \text{(5o)}\\
& && \text{(5)}
\end{aligned}
$$

The active and reactive power balance at each bus ($n \in \mathcal{N}$) are modeled in (5c)

and (5d). The active power balance at node n reflects the active power generation of all generators at the node ($\mathcal{G}(n)$), active power demand, shunt conductance (G_n^S) with bus voltage (v_n), power injected to branches with origin or destination terminals at node n ($\mathcal{B}(n)$). The reactive power balance is defined similarly with shunt admittance (B_n^S). Power flow and thermal limit constraints for all branches ($\mathcal{B}$, including lines and transformers) are captured in (5e), (5f), and (5g). The active or reactive power of lines and transformers are calculated from voltage magnitudes (v), voltage angles (θ), and coefficients related to device characteristics. The index i indicates whether the bus is the origin or the destination for the branch e ($i = 1$ for origin and $i = 2$ for destination). The voltage magnitudes v_1 and v_2 are at the origin and destination buses, respectively. The voltage angle for branch e (θ_e) is calculated from difference of origin and destination bus voltage angles. As described in (5g), the active and reactive power of lines and transformers are constrained by a squared summation of bus voltages and penalty terms. For thermal limits, R is the

thermal rating for the line or transformer at the branch e.

$$\min_{P_{l,t},x_t=\{P_{g,t},Q_{g,t},v_{n,t},\theta_{e,t},\sigma_t\}} \sum_{t=1}^{T} f_t(P_{l,t},x_t) \tag{6a}$$

$$s.t. \quad f_t(P_{l,t},x_t) = GC_t(x_t) + PC_t(P_{l,t},x_t) - R_t(P_{l,t}) \tag{6b}$$

$$P_{a,n,t}(x_t) - \sum_{l\in\mathcal{L}(n)} P_{l,t} = \sigma_{a,n,t} \quad \forall\, n\in\mathcal{N}, t\in[1,T] \tag{6c}$$

$$Q_{r,n,t}(x_t) = \sigma_{r,n,t} \quad \forall\, n\in\mathcal{N}, t\in[1,T] \tag{6d}$$

$$P_{e_i,t} = P_{a,e_i,t}(x_t) \quad \forall\, e\in\mathcal{B}, i\in\{1,2\}, t\in[1,T] \tag{6e}$$

$$Q_{e_i,t} = P_{r,e_i,t}(x_t) \quad \forall\, e\in\mathcal{B}, i\in\{1,2\}, t\in[1,T] \tag{6f}$$

$$P_{e_i,t}^2 + Q_{e_i,t}^2 \le (Rv_{e_i,t} + \sigma_{e_i,t})^2 \quad \forall\, e\in\mathcal{B}, i\in\{1,2\}, t\in[1,T] \tag{6g}$$

$$GC_t(x_t) = \sum_{g\in\mathcal{G}} GC_{g,t} \quad \forall\, t\in[1,T] \tag{6h}$$

$$PC_t(x_t) = C(\sigma_t) \quad \forall\, t\in[1,T] \tag{6i}$$

$$P_g^{min} \le P_{g,t} \le P_g^{max} \quad \forall\, g\in\mathcal{G}, t\in[1,T] \tag{6j}$$

$$Q_g^{min} \le Q_{g,t} \le Q_g^{max} \quad \forall\, g\in\mathcal{G}, t\in[1,T] \tag{6k}$$

$$P_{e_i}^{min} \le P_{e_i,t} \le P_{e_i}^{max} \quad \forall\, e\in\mathcal{B}, i\in\{1,2\}, t\in[1,T] \tag{6l}$$

$$Q_{e_i}^{min} \le Q_{e_i,t} \le Q_{e_i}^{max} \quad \forall\, e\in\mathcal{B}, i\in\{1,2\}, t\in[1,T] \tag{6m}$$

$$v_n^{min} \le v_{n,t} \le v_n^{max} \quad \forall\, N\in\mathcal{N}, t\in[1,T] \tag{6n}$$

$$\theta_n^{min} \le \theta_{n,t} \le \theta_n^{max} \quad \forall\, N\in\mathcal{N}, t\in[1,T] \tag{6o}$$

$$P_l^{min} \le P_{l,t} \le P_l^{max} \quad \forall\, t\in[1,T] \tag{6p}$$

$$-LR \le P_{l,t} - P_{l,t+1} \le LR \quad \forall\, l\in\mathcal{L}, t\in[1,T-1] \tag{6q}$$

$$-GR_g \le P_{g,t} - P_{g,t+1} \le GR_g \quad \forall\, g\in\mathcal{G}, t\in[1,T-1] \tag{6r}$$

$$PR_t = E_t(P_{l,t}) \quad \forall\, t\in[1,T] \tag{6s}$$

$$R_t(P_{l,t}) = R_u PR_t \quad \forall\, t\in[1,T] \tag{6t}$$

$$D \le \sum_{t=1}^{T} PR_t \le C \tag{6u}$$

(6)

As shown in Equation (6), the demand bidding (in AC OPF) model can be generalized as a minimization problem where the objective function ($f_t(P_{l,t},x_t)$) is a summation of generation costs, penalty costs, and production revenue over the whole time horizon (6b). Since the problem is MP, all variables are also indexed by time t. Equations (6d) to (6o) are the AC OPF constraints (except from active power balance) in MP form. The active power balance (6c) is similar to the regular balance (5c), except that bidding load/plant power consumption $P_{l,t}$ on bus n is included ($l\in\mathcal{L}(n)$); also, the reader should note that the maximum number of bidding loads on bus n is 1 in this case study. Ramp rate limits for the bidding plant and generator power levels ($P_{l,t}$ and $P_{g,t}$ respectively) are added separately as (6q) and (6r). Specifically, LR is the ramp rate limit for the bidding plant $l\in\mathcal{L}$ (same for all bidding loads/plants) obtained from specific plant data, and GR is the ramp rate limit for each generator $g\in\mathcal{G}$. The bidding plant production rate is calcu-

lated from plant power consumption (6s) with production efficiency. In other words, bidding plant production rate can be defined as a function of bidding plant power $PR_t = E_t(P_{l,t})$, and can be simplified to $PR_t = \eta P_{l,t}$ if the production efficiency is a linear coefficient (η in unit of production per unit energy, *e.g.*, ton/MWh). The total production revenue can be calculated from total production and unit revenue R_u (with unit of dollars earned per unit production, *e.g.*, $/ton). The total production is the integral of production rates over time, which should be constrained by demand (D) and capacity (C) as seen in (6u). This constraint ensures that the production always satisfies customer demand, and is less than the maximum capacity limit of the facility. This is of paramount importance for the bidding entities because their primary goal is to satisfy customer demand rather than keep the power balance.

The MP AC OPF with demand bidding model was implemented in Julia (v1.9) and solved using the IPOPT (version 3.14.13) solver[24,25]. The runtime varies from less than ten minutes to about two hours. Since the formulation is nonlinear and nonconvex, the solver might enter different branches of the algorithm, so no runtime prediction can be made.

Structure of generation cost function

For each generator g, the cost of power generation is described using a piecewise linear function that relates the generation cost to the power generation level. The piecewise-linear functions are described via a set of $npairs$ pairs of parameters $[CostP_{g,h}, CostC_{g,h}]$. The power generated by generator g at time point t can be expressed as

$$G_{g,t} = \sum_{h=1}^{npairs} CostP_{g,h} \cdot th_h \quad s.t. \sum_{h=1}^{npairs} th_h = 1 \tag{7a}$$

while the generation cost $GC_{g,t}$ is computed as:

$$GC_{g,t} = \sum_{h=1}^{npairs} CostC_{g,h} \cdot th_h \tag{7b}$$

(7)

The unit generation cost parameters are presented as pairs ($CostP_g$ and $CostC_g$). In this system, the two parameters have either two or three points. For example, $CostP_g = [G^{LB}, G^{UB}]$ (G^{LB}, G^{UB} are bounds for generator powers) and $CostC_g = [0, 0]$ for the zero-cost generators. For other generators, $CostC_g = [GC_u^{LB}, GC_u^{UB}]$, which means the cost of power generation increases linearly from GC_u^{LB} to GC_u^{UB} as the power levels change from G^{LB} to G^{UB}, as shown in Figure 10. In addition, for some generators, $CostP_g = [G^{LB}, G^M, G^{UB}]$ and $CostC_g = [GC_u^{LB}, GC_u^M, GC_u^{UB}]$, where they have piecewise linear generation costs, meaning that the generation cost increases linearly on two generation segments $[G^{LB}, G^M]$ and $[G^M, G^{UB}]$.

To demonstrate the how generation cost is calculated, we look at the following example where $CostP_g = [50, 200, 250](MW)$ and $CostC_g = [10, 100, 200](\$/MWh)$. With generation rate $G_{g,t}$, th_h (th_1, th_2, th_3 in this case) can be calculated from (7a). If $G_{g,t} = 200MW$, $th_1 = 0, th_2 = 1, th_3 = 0$ is the solution. With this solution, generation cost $GC_{g,t}$ (for the hour t) can be obtained from (7b). In this case,

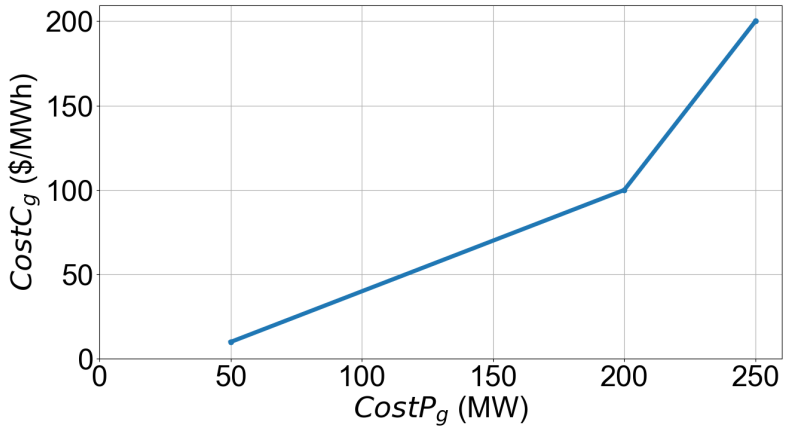

Figure 10: The piecewise linear generation cost function for a sample generator with $CostP_g = [50, 200, 250](MW)$ and $CostC_g = [10, 100, 200](\$/MWh)$.

$GC_{g,t} = 100\$/MWh$. As seen in Figure 10, the generation cost varies linearly between $GC_u^{LB} = 10\$/MWh$ and $GC_u^M = 100\$/MWh$ as generation rate ranges from $G^{LB} = 50MW$ to $G^M = 200MW$. As generation rate changes from $G^M = 200MW$ to $G^{UB} = 250MW$, the generation cost increases from $GC_u^M = 100\$/MWh$ to $GC_u^{UB} = 200\$/MWh$ at a higher linear rate. In other words, the parameters provide the end and elbow points of the generation cost functions.

Generation cost scenarios

In the 2000-bus system, 118 zero-cost generators can produce electricity at no cost ($CostC_g = [0, 0]$), reflecting renewable energy generators. We also examined the effect of varying unit generation costs of those zero-cost generators. The values of $CostC_g$ depend on the characteristics of the generators. Aside from the zero-cost generators, GC_u^{LB} ranges from about $350\,\$/MWh$ to $9,300\,\$/MWh$ while GC_u^{UB} varies from around $630\,\$/MWh$ to $22,900\,\$/MWh$. In the case study, several sets of the unit generation costs ($CostC_g$) of zero-cost generators are examined: $[0, 0], [0, 100], [0, 1000], [0, 10000]$. The case of $[0, 100]$ is similar to $[0, 0]$, and in the case of $[0, 10000]$, all "zero-cost" generators are operating at lower limits almost at all times. Thus, in this work, only results of $[0, 0]$ and $[0, 1000]$ are discussed in the RESULTS Section.

Bidding entity characteristics

In previous work[13], a chlor-alkali plant was used as the bidding entity for model validation. The plant characteristics are adopted in this work such that the plant closely resembles a large industrial load. The key plant parameters are summarized in Table 1. Bidding entity parameters. The product demand and power limits represent the scale of the plant. Note for this plant, 10% of overproduction is allowed and used as the upper limit of total daily production. Aside from the lower and upper limits of the plant power, the production ramping limit (limiting how fast the production power can ramp up or down) and system efficiency (unit production per unit electricity consumed) are also important plant power operating parameters.

In addition, the unit production revenue (derived from production system efficiency and published product price) is important for the welfare calculation.

Table 1. Bidding entity parameters

Parameter	Value	Unit	Definition
P_l^{min}	35	MW	Lower limit of plant power
P_l^{max}	70	MW	Upper limit of plant power
LR	35.5	MW/h	Production ramping limit
η	0.5	t Cl_2 /MWh	Production system efficiency
R_u	100	$ /MWh	Unit production revenue
D	550	t Cl_2	Daily demand of chlorine
C	605	t Cl_2	Maximum daily production of chlorine

Resource availability

Lead contact

Requests for further information and resources should be directed to and will be fulfilled by the lead contact, Michael Baldea (mbaldea@che.utexas.edu).

Materials availability

This study did not generate new materials.

Data and code availability

- Our source code is currently in the process of being released for public use under an open-source license and will be made available publicly shortly.
- Any additional information required to reanalyze the data reported in this paper is available from the lead contact upon request.

Supplemental information index

Acknowledgments

This work was partially performed under the auspices of the U.S. Department of Energy by Lawrence Livermore National Laboratory under contract DE–AC52–07NA27344. MB acknowledges support from EPIXC, a US Department of Energy Clean Energy Manufacturing Innovation Institute (award DE-EE0010725).

Author contributions

Conceptualization, C.G.P. and M.B.; methodology, C.G.P., X.T., M.B. and R.B.; investigation, X.T., C.G.P., and M.B.; writing – original draft, X.T.; writing – review & editing, C.G.P., X.T., R.B. and M.B.; funding acquisition, C.G.P. and M.B.; resources, C.G.P.; supervision, M.B. and C.G.P.

Declaration of interests

The authors declare no competing interests.

References

1. Bouckaert, S., Pales, A. F., McGlade, C., Remme, U., Wanner, B., Varro, L., D'Ambrosio, D., and Spencer, T. (2021). Net zero by 2050: A roadmap for the global energy sector.

2. DOE, U. Enabling modernization of the electric power system technology assessment — electric energy storage. https://www.energy.gov/quadrennial-technology-review-2015, last retrieved 05/17/2022 (2015).

3. Lazard. Lazard's levelized cost of storage analysis (2023). file:///C:/Users/Administrator/Downloads/lazards-lcoeplus-april-2023.pdf.

4. Cembalest, M. Growing pains: The renewable transition in adolescence (2023). https://privatebank.jpmorgan.com/gl/en/insights/investing/eotm/annual-energy-paper.

5. U.S. Dept of Energy. Benefits of demand response in electricity markets and recommendations for achieving them, report to congress under the energy policy act of 2005 section 1252 (2006). https://www.energy.gov/oe/downloads/benefits-demand-response-electricity-markets-and-recommendations-achieving-them-report

6. Vahid-Ghavidel, M., Javadi, M. S., Gough, M., Santos, S. F., Shafie-Khah, M., and Catalao, J. P. (2020). Demand response programs in multi-energy systems: A review. Energies *13*, 4332.

7. Ferreira, H. L., Garde, R., Fulli, G., Kling, W., and Lopes, J. P. (2013). Characterisation of electrical energy storage technologies. Energy *53*, 288–298. https://www.sciencedirect.com/science/article/pii/S0360544213001515. doi:10.1016/j.energy.2013.02.037.

8. Albadi, M. H., and El-Saadany, E. F. Demand response in electricity markets: An overview. In: *2007 IEEE power engineering society general meeting*. IEEE (2007):(1–5).

9. Li, Y.-C., and Hong, S. H. (2016). Real-time demand bidding for energy management in discrete manufacturing facilities. IEEE Transactions on Industrial Electronics *64*, 739–749.

10. Ruan, G., Zhong, H., Shan, B., and Tan, X. (2020). Constructing demand-side bidding curves based on a decoupled full-cycle process. IEEE Transactions on Smart Grid *12*, 502–511.

11. Mohsenian-Rad, H. (2014). Optimal demand bidding for time-shiftable loads. IEEE Transactions on Power Systems *30*, 939–951.

12. Kohansal, M., and Mohsenian-Rad, H. (2015). Price-maker economic bidding in two-settlement pool-based markets: The case of time-shiftable loads. IEEE Transactions on Power Systems *31*, 695–705.

13. Tang, X., O'Neill, R., Hale, E., Baldick, R., and Baldea, M. (2024). Demand bidding vs. demand response for industrial electrical loads. Computers & Chemical Engineering (108768).

14. Midcontinent ISO. MISO Business Practices Manuals, BPM-26, Demand Response. https://www.misoenergy.org/legal/rules-manuals-and-agreements/business-practice-manuals/, last retrieved 5/6/2024 (2024).

15. Birchfield, A. B., Xu, T., Gegner, K. M., Shetye, K. S., and Overbye, T. J. (2016). Grid structural characteristics as validation criteria for synthetic networks. IEEE Transactions on power systems *32*, 3258–3265.

16. Xu, T., Birchfield, A. B., Gegner, K. M., Shetye, K. S., and Overbye, T. J. (2017). Application of large-scale synthetic power system models for energy economic studies.

17. Li, H., Bornsheuer, A. L., Xu, T., Birchfield, A. B., and Overbye, T. J. Load modeling in synthetic electric grids. In: *2018 IEEE Texas Power and Energy Conference (TPEC)*. IEEE (2018):(1–6).

18. Li, H., Yeo, J. H., Bornsheuer, A. L., and Overbye, T. J. (2020). The creation and validation of load time series for synthetic electric power systems. IEEE Transactions on Power Systems *36*, 961–969.

19. ARPA-E. SCOPF problem formulation: Challenge 1 (2019). https://gocompetition.energy.gov/sites/default/files/SCOPF_Problem_Formulation__Challenge_1_20190412.pdf.

20. Petra, C. G., and Aravena, I. (2023). A surrogate-based asynchronous decomposition technique for realistic security-constrained optimal power flow problems. Operations Research *71*, 2015–2030.

21. Maharjan, S., Zhu, Q., Zhang, Y., Gjessing, S., and Basar, T. (2013). Dependable demand response management in the smart grid: A Stackelberg game approach. IEEE Transactions on Smart Grid *4*, 120–132.

22. Yoon, S.-G., Choi, Y.-J., Park, J.-K., and Bahk, S. (2015). Stackelberg-game-based demand response for at-home electric vehicle charging. IEEE Transactions on Vehicular Technology *65*, 4172–4184.

23. Shakrina, Y., and Margossian, H. (2021). A Stackelberg game-inspired model of real-time economic dispatch with demand response. International Transactions on Electrical Energy Systems *31*, e13076.

24. Wächter, A., and Biegler, L. T. (2006). On the implementation of an interior-point filter line-search algorithm for large-scale nonlinear programming. Mathematical programming *106*, 25–57.

25. Duff, I. S. (2004). Ma57—a code for the solution of sparse symmetric definite and indefinite systems. ACM Transactions on Mathematical Software (TOMS) *30*, 118–144.